

Search for K^+ decays to a lepton and invisible particles

Nicolas Lurkin^{a,*}

^{a,1}*Centre for Cosmology, Particle Physics and Phenomenology, Université catholique de Louvain, Louvain-la-Neuve, Belgium*

E-mail: nicolas.lurkin@cern.ch

Searches for heavy neutral leptons N in the $K^+ \rightarrow e^+N$ and $K^+ \rightarrow \mu^+N$ decay channels using the dataset collected by the NA62 experiment at CERN between 2016-2018 are presented. Upper limits on the corresponding mixing matrix elements are reported at the level of $O(10^{-9})$ and $O(10^{-8})$, respectively. This represents an improvement of at least an order of magnitude on previous measurement, as well as an extension to higher masses than previously covered. Related searches set upper limits on the rate of the $K^+ \rightarrow \mu^+\nu\nu\bar{\nu}$ and $K^+ \rightarrow \mu^+\nu X$ decay channels, with X an invisible scalar or vector boson.

*** *The 22nd International Workshop on Neutrinos from Accelerators (NuFact2021)* ***

*** *6–11 Sep 2021* ***

*** *Cagliari, Italy* ***

¹For the NA62 Collaboration: A. Akmete, R. Aliberti, F. Ambrosino, R. Ammendola, B. Angelucci, A. Antonelli, G. Anzivino, R. Arcidiacono, T. Bache, A. Baeva, D. Baigarashev, L. Bandiera, M. Barbanera, J. Bernhard, A. Biagioni, L. Bician, C. Biino, A. Bizzeti, T. Blazek, B. Bloch-Devaux, P. Boboc, V. Bonaiuto, M. Boretto, M. Bragadireanu, A. Briano Olvera, D. Britton, F. Brizioli, M.B. Brunetti, D. Bryman, F. Bucci, T. Capussela, J. Carmignani, A. Ceccucci, P. Cenci, V. Cerny, C. Cerri, B. Checucci, A. Conovaloff, P. Cooper, E. Cortina Gil, M. Corvino, F. Costantini, A. Cotta Ramusino, D. Coward, P. Cretaro, G. D'Agostini, J. Dainton, P. Dalpiaz, H. Danielsson, M. D'Errico, N. De Simone, D. Di Filippo, L. Di Lella, N. Doble, B. Dobrich, F. Duval, V. Duk, D. Emelyanov, J. Engelfried, T. Enik, N. Estrada-Tristan, V. Falaleev, R. Fantechi, V. Fascianelli, L. Federici, S. Fedotov, A. Filippi, R. Fiorenza, M. Fiorini, O. Frezza, J. Fry, J. Fu, A. Fucci, L. Fulton, E. Gamberini, L. Gagnon, G. Georgiev, S. Ghinescu, A. Gianoli, M. Giorgi, S. Giudici, F. Gonnella, K. Gorbhanov, E. Goudzovski, C. Graham, R. Guida, E. Gushchin, F. Hahn, H. Heath, J. Henshaw, Z. Hives, E.B. Holzer, T. Husek, O. Hutanu, D. Hutchcroft, L. Iacobuzio, E. Iacopini, E. Imbergamo, B. Jenner, J. Jerhot, R.W. Jones, K. Kampf, V. Kekelidze, D. Kerebay, S. Kholodenko, G. Khorauli, A. Khotyantsev, A. Kleimenova, A. Korotkova, M. Koval, V. Kozhuharov, Z. Kucerova, Y. Kudenko, J. Kunze, V. Kurochka, V. Kurshetsov, G. Lanfranchi, G. Lamanna, E. Lari, G. Latino, P. Laycock, C. Lazzeroni, M. Lenti, G. Lehmann Miotto, E. Leonardi, P. Lichard, L. Litov, P. Lo Chiato, R. Lollini, D. Lomidze, A. Lonardo, P. Lubrano, M. Lupi, N. Lurkin, D. Madigozhin, I. Mannelli, A. Mapelli, F. Marchetto, R. Marchevski, S. Martellotti, P. Massarotti, K. Massri, E. Maurice, A. Mazzolari, M. Medvedeva, A. Mefodev, E. Menichetti, E. Migliore, E. Minucci, M. Mirra, M. Misheva, N. Molokanova, M. Moulson, S. Movchan, M. Napolitano, I. Neri, F. Newson, A. Norton, M. Noy, T. Numao, V. Obraztsov, A. Okhotnikov, A. Ostankov, S. Padolski, R. Page, V. Palladino, I. Panichi, A. Parenti, C. Parkinson, E. Pedreschi, M. Pepe, M. Perrin-Terrin, L. Peruzzo, P. Petrov, Y. Petrov, F. Petrucci, R. Piandani, M. Piccini, J. Pinzino, I. Polenkevich, L. Pontisso, Yu. Potrebenikov, D. Protopopescu, M. Raggi, M. Reyes Santos, M. Romagnoni, A. Romano, P. Rubin, G. Ruggiero, V. Ryjov, A. Sadovsky, A. Salamon, C. Santoni, G. Saracino, F. Sargeni, S. Schuchmann, V. Semenov, A. Sergi, A. Shaikhiev, S. Shkarovskiy, M. Soldani, D. Soldi, M. Sozzi, T. Spadaro, F. Spinella, A. Sturgess, V. Sugonyaev, J. Swallow, A. Sytov, G. Tinti, A. Tomczak, S. Trilov, M. Turisini, P. Valente, B. Velghe, S. Venditti, P. Vicini, R. Volpe, M. Vormstein, H. Wahl, R. Wanke, V. Wong, B. Wrona, O. Yushchenko, M. Zamkovsky, A. Zinchenko.

*Speaker

© Copyright owned by the author(s) under the terms of the Creative Commons Attribution-NonCommercial-NoDerivatives 4.0 International License (CC BY-NC-ND 4.0).

<https://pos.sissa.it/>

1. Introduction

All Standard Model (SM) fermions except neutrinos are known to exhibit right-handed chirality. The existence of right-handed neutrinos, or heavy neutral leptons (HNLs), is hypothesised in many SM extensions in order to generate non-zero masses of the SM neutrinos via the seesaw mechanism. For example, the Neutrino Minimal Standard Model simultaneously accounts for dark matter, baryogenesis, and neutrino masses and oscillations by postulating two HNLs in the MeV–GeV mass range and a third HNL, a dark matter candidate, at the keV mass scale [1].

Mixing between HNLs and active neutrinos gives rise to HNL production in decays of SM particles and decays of HNLs into SM particles. The branching fraction for decay for the decay $K^+ \rightarrow \ell^+ N$ ($\ell = e, \mu$) takes the form [2]:

$$\mathcal{B}(K^+ \rightarrow \ell^+ N) = \mathcal{B}(K^+ \rightarrow \ell^+ \nu) \cdot \rho_\ell(m_N) \cdot |U_{\ell 4}|^2, \quad (1)$$

where N denotes an HNL, $\mathcal{B}(K^+ \rightarrow \ell^+ \nu)$ is the measured branching fraction of the equivalent SM decay, $|U_{\ell 4}|$ is the mixing parameter, m_N is the HNL mass, and $\rho_\ell(m_N)$ is the kinematic factor:

$$\rho_\ell(m_N) = \frac{(x+y) - (x-y)^2}{x(1-x)^2} \cdot \lambda^{1/2}(1, x, y), \quad (2)$$

with $x = (m_\ell/m_K)^2$, $y = (m_N/m_K)^2$ and $\lambda(a, b, c) = a^2 + b^2 + c^2 - 2(ab + bc + ac)$. Numerically, the product $\mathcal{B}(K^+ \rightarrow \ell^+ \nu) \cdot \rho_\ell(m_N)$ is $\mathcal{O}(1)$ over most of the allowed m_N range. It reduces to $\mathcal{B}(K^+ \rightarrow \ell^+ \nu) = 1.582(7) \times 10^{-5}$ for $m_N = 0$ and drops to zero at the kinematic limit $m_N = m_K - m_\ell$. The positron channel benefits from a $\mathcal{O}(10^5)$ enhancement due to the relaxation of the helicity suppression with respect to the SM channel. Conservative assumptions on the mixing parameter $|U_{\ell 4}|^2$ allow the HNL to be treated as a stable particle for production searches.

A new light gauge boson has been proposed as an explanation to the muon g-2 anomaly [3]. A particular scenario, which also accommodates dark matter (DM) freeze-out, involves a scalar or vector hidden sector mediator X coupling preferentially to the muon. For a mediator with mass $m_X < m_K - m_\mu$, the decay $K^+ \rightarrow \mu^+ \nu X$ could proceed with an estimated branching fraction of $\mathcal{O}(10^{-8})$, followed by a prompt decay of the mediator with a sizeable invisible branching fraction [4]. In the light DM freeze-out model, the $X \rightarrow \chi \bar{\chi}$ decay is expected, where χ is the DM particle.

The $K^+ \rightarrow \mu^+ \nu \nu \bar{\nu}$ decay is expected within the SM with a branching fraction of $\mathcal{B}_{\text{SM}} = 1.62 \times 10^{-16}$ [5] which is experimentally out of reach. The strongest upper limit to date has been established by the BNL-E949 experiment at $\mathcal{B}(K^+ \rightarrow \mu^+ \nu \nu \bar{\nu}) < 2.4 \times 10^{-6}$ at 90% CL [6].

The NA62 experiment [7], located in the CERN north area, uses a decay-in-flight technique to study K^+ decays. The primary 400 GeV/c proton beam of the CERN SPS impinges on a beryllium target to produce a secondary beam of unseparated hadrons. This beam is composed of positively charged pions (70%), protons (24%) and kaons (6%) with a central momentum of 75 GeV/c and a 1% (rms) momentum spread. A differential Cherenkov detector (KTAG) tags incoming kaons in the beam, and their momenta is measured by the beam spectrometer (GTK). The kaons are then left to decay in a ~ 75 m long fiducial volume (FV) under vacuum. The momenta of the charged decay products are measured by a STRAW spectrometer after the FV. Powerful particle identification (PID) comes from the combination of a Ring Imaging Cherenkov detector (RICH), a liquid krypton calorimeter (LKr), and a muon detector system (MUV). In addition, a hermetic set

of photon detectors surround the FV. Two charged hodoscopes are located between the RICH and the LKr, and provide trigger signals and time measurement.

This document reports a study of $K^+ \rightarrow \ell^+ N$, $K^+ \rightarrow \ell^+ \nu X$, and $K^+ \rightarrow \mu^+ \nu \nu \bar{\nu}$ decays using the dataset collected during the 2016–2018 period, where more than 1×10^{12} K^+ decays were recorded. The N particle is interpreted as a HNL, and results are presented in terms of upper limits on the mixing parameter $|U_{\ell 4}|^2$ under the assumption that the HNL lifetime exceeds 50 ns. The X particle is interpreted as a new boson, either vector or scalar, and results are presented in terms of upper limits on the $K^+ \rightarrow \ell^+ \nu X$ branching fraction.

2. Event selection

Due to the similarity of their final state, each of the signal decays considered is selected from single-track events samples. These samples are constructed by requesting a single positively charged track reconstructed in the STRAW spectrometer, in the geometrical acceptance of the LKr, CHOD, and MUV3 detector, and identified as leptons by the PID detectors. Further separation between positrons and muons is performed using additional requirements. Positrons are required to have momentum (p) between 5 GeV/ c and 30 GeV/ c , the ratio between the energy deposited in the LKr (E) to the momentum p must be in the range 0.92–1.08, and leave no hit in the muon detector consistent in space and time with the reconstructed track. Muons are required to have momenta between 5 GeV/ c and 70 GeV/ c , the ratio $E/p < 0.2$, and a hit in the muon detector consistent in space and time with the reconstructed track. For tracks below 30 GeV/ c , a RICH-based particle identification algorithm was also applied to distinguish between positrons and muons. Backgrounds from beam pions are suppressed by requiring a positive kaon signal in the KTAG, consistent in time with the lepton. The K^+ track reconstructed in the GTK is matched with the lepton track using a discriminant based on the time difference and the closest distance of approach. Pile-up background resulting from kaon decay in the beam line is reduced by applying geometrical constraints on the longitudinal position of the reconstructed vertex, defined as the closest point of approach between the K^+ and lepton track, in the FV. The condition applied varies as a function of the angle between the K^+ momentum in the lab frame and the lepton momentum in the K^+ rest frame. Finally, backgrounds from multi-body K^+ decays are suppressed by veto conditions imposed on other tracks reconstructed by the STRAW spectrometer, additional energy deposits in the LKr, energy deposits in the photon veto system, and additional signals in the CHOD.

The two main measured quantities in the selected events are the reconstructed momenta P_K and P_ℓ of the incoming K^+ and of the outgoing lepton, respectively. They can be combined into the squared missing mass $m_{\text{miss}}^2 = P_K^2 - P_\ell^2$, which is plotted in Fig. 1 for the electron case (left) and the muon case (right). The signal from the SM $K^+ \rightarrow \ell^+ \nu$ decays is peaked at $m_{\text{miss}}^2 = 0$. Defining the SM signal region as $|m_{\text{miss}}^2| < 0.01 \text{ GeV}^2/c^4$, the selection yields 3.495×10^6 $K^+ \rightarrow e^+ \nu$ candidates and 2.19×10^9 $K^+ \rightarrow \mu^+ \nu$ candidates. The m_{miss}^2 distribution exhibits a sharp increase around $m_{\text{miss}}^2 = 0.13 \text{ GeV}^2/c^4$, due to background from beam pion decays. This threshold depends on the on the maximum positron momentum. Therefore, an "auxilliary" selection with lower selection efficiency was defined imposing a maximum positron momentum of $< 20 \text{ GeV}$, allowing the high m_{miss}^2 region to be probed without this overwhelming background.

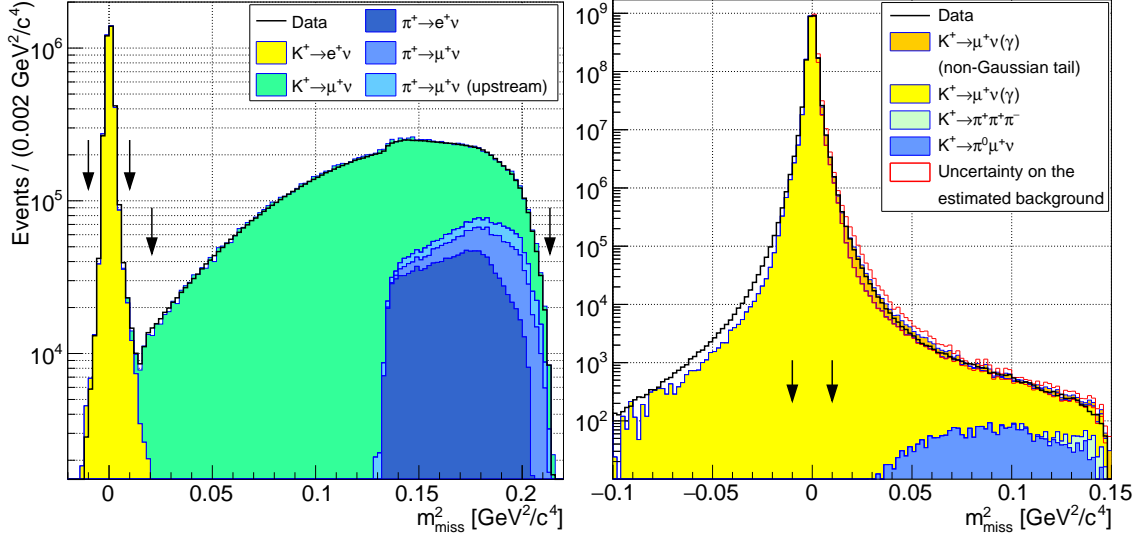


Figure 1: Reconstructed m_{miss}^2 distribution of $K^+ \rightarrow e^+ \nu$ (left) and $K^+ \rightarrow \mu^+ \nu$ (right) candidates in data (black line) and simulated events (coloured areas).

3. Measurement principle and result

Any $K^+ \rightarrow \ell^+ N$ signal will appear as a sharp peak in the m_{miss}^2 distribution. A scan of the m_{miss}^2 spectrum was performed opening windows of width $1.5\sigma_m$, where σ_m is the m_{miss}^2 resolution at the given value of m_N . The mass range covered and the step between windows is variable: σ_m in the range 144-462 MeV/ c^2 for the positron case, 1MeV/ c^2 in the range 200-300 MeV/ c^2 and 0.5MeV/ c^2 in the range 300-384 MeV/ c^2 for the muon case. For each window, the background is evaluated by a 2nd order polynomial fit to the data in the sideband $1.5\sigma_m < |m_{\text{miss}}^2 - m_N| < 11.25\sigma_m$. The auxiliary selection is used in the positron case when close to the beam pion decay threshold to ensure good fits are obtained. The limit on the number of $K^+ \rightarrow \ell^+ N$ signals events observed in each window is obtained by the CLs method using the number of events observed, the expected background, and the uncertainty on the expected background. The limits obtained are shown in Fig.2 for the positron case (left) and the muon case (right). The results are also interpreted as limits on the mixing parameters $|U_{e4}|^2$ and $|U_{\mu 4}|^2$, which are compared to previous limits in Fig.3.

The m_{miss}^2 distribution of the $K^+ \rightarrow \ell^+ \nu X$ and $K^+ \rightarrow \mu^+ \nu \nu \bar{\nu}$ decays exhibit a broad spectrum of large positive m_{miss}^2 . In both cases the search is performed in a region $m_{\text{miss}}^2 > m_0^2$, where m_0^2 is optimized to extract the strongest limit. In the $K^+ \rightarrow \ell^+ \nu X$ case, the search is performed in 37 m_X hypotheses equally spaced between 10-370 MeV/ c^2 , in both the scalar and vector models. Upper limits on the branching fraction are set using the CLs method, with the expected background and its uncertainty evaluated using simulated events. The limits for $K^+ \rightarrow \ell^+ \nu X$ are shown in Fig.3 (right). The limits obtained in the scalar model are stronger due to the larger mean m_{miss}^2 value. In the search for the $K^+ \rightarrow \mu^+ \nu \nu \bar{\nu}$ decay, 6894 events are observed in the signal region, with an expected background of 7549 ± 928 events. This leads to an observed limit of $\mathcal{B}(K^+ \rightarrow \mu^+ \nu \nu \bar{\nu}) < 1.0 \times 10^{-6}$ at 90% CL, improving on the previous most stringent limit by a factor of 2.4 in a complementary range of m_{miss}^2 .

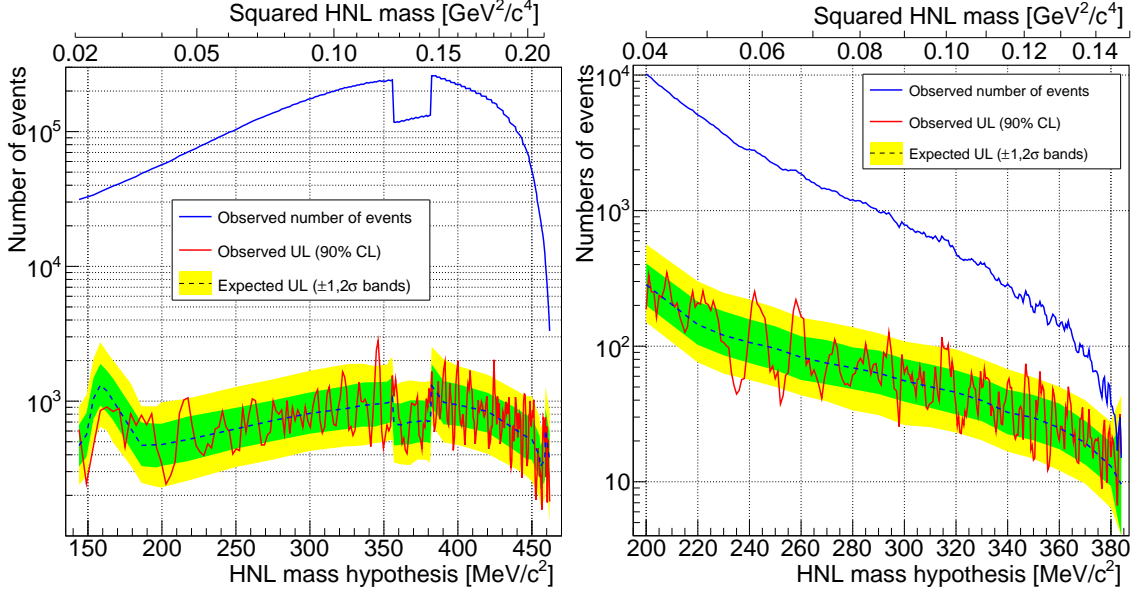


Figure 2: The observed number of events (blue line), the observed upper limit at 90% CL (red line), and the expected limit (black dashed line) with its associated 1σ and 2σ bands (green, yellow coloured areas) for the $K^+ \rightarrow e^+ N$ (left) and $K^+ \rightarrow \mu^+ N$ (right) searches.

4. Summary

This document reports four world-leading measurements by the NA62 experiment. Improved limits at the level of 10×10^{-9} (10×10^{-8}) were set on the HNL mixing parameter $|U_{e4}|^2$ ($|U_{\mu 4}|^2$) in the mass range $144\text{--}462 \text{ MeV}/c^2$ ($200\text{--}384 \text{ MeV}/c^2$). These are the world's best limits in this mass range for $|U_{e4}|^2$, and above $300 \text{ MeV}/c^2$ for $|U_{\mu 4}|^2$. The first ever limits were set on the branching fraction of the $K^+ \rightarrow \ell^+ \nu X$ decay, with X either a scalar or vector boson with mass in the range $10\text{--}370 \text{ MeV}/c^2$ that decays to invisible particles. Finally, the limit of $\mathcal{B}(K^+ \rightarrow \mu^+ \nu \nu \bar{\nu}) < 1.0 \times 10^{-6}$ was set at 90% CL, improving on earlier limits and probing a complementary region of m_{miss}^2 .

References

- [1] T. Asaka, M. Shaposhnikov, Phys. Lett. B 620 (2005) 17.
- [2] R. Shrock, Phys. Lett. B 96 (1980) 159; Phys. Rev. D 24 (1981) 1232.
- [3] S.N. Gninenko, N.V. Krasnikov, Phys. Lett. B 513 (2001) 119.
- [4] G. Krnjaic, et al., Phys. Rev. Lett. 124 (2020) 041802.
- [5] D. Gorbunov, A. Mitrofanov, J. High Energy Phys. 1610 (2016) 039.
- [6] A.V. Artamonov, et al., Phys. Rev. D 94 (2016) 032012.
- [7] E. Cortina Gil, et al., J. Instrum. 12 (2017) P05025.

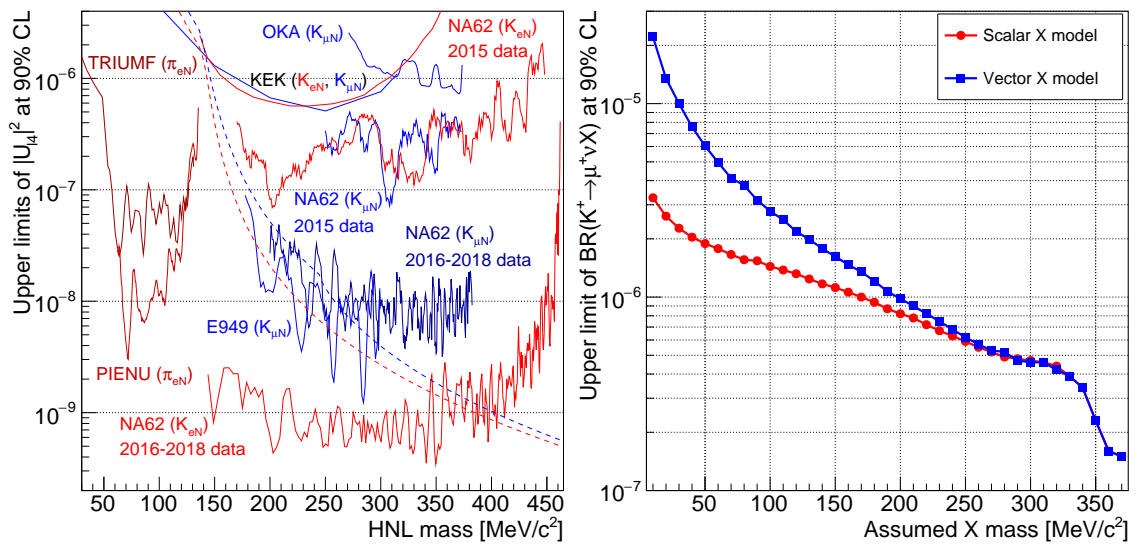


Figure 3: Left: Observed upper limits at 90 % CL of $|U_{e4}|^2$ (red solid lines) and $|U_{\mu 4}|^2$ (blue solid lines) compared to the existing world knowledge. The lower boundaries imposed by the BBN constraint are shown by the dashed lines. Right: observed upper limit on $\mathcal{B}(K^+ \rightarrow \ell^+ \nu X)$ as a function of m_X , assuming a scalar (red points) or vector (blue points) X boson.